KJVR
Korean Journal of Veterinary Research

Case Report

Medical Imaging

pISSN 2466-1384 · eISSN 2466-1392
Korean J Vet Res 2023;63(4):e39
https://doi.org/10.14405/kjvr.20230041

*Corresponding author:
Kija Lee
Department of Veterinary Medical Imaging, College of Veterinary Medicine, Kyungpook National University, 80 Daehak-ro, Buk-gu, Daegu 41566, Korea
Tel: +82-53-950-5961
E-mail: leekj@knu.ac.kr
https://orcid.org/0000-0002-4649-809X

Conflict of interest:
The authors declare no conflict of interest.

Received: Sep 19, 2023
Revised: Nov 10, 2023
Accepted: Nov 19, 2023

Computed tomography and magnetic resonance imaging features of suspected transitional cell carcinoma lesions involving the bladder, prostate, and urethra in a dog: a case report

Wooseok Jin[1], Sang-Kwon Lee[1], Seulgi Bae[2], Taeho Oh[2], Kija Lee[1,*]

[1]Department of Veterinary Medical Imaging, College of Veterinary Medicine, Kyungpook National University, Daegu 41566, Korea
[2]Department of Veterinary Internal Medicine, College of Veterinary Medicine, Kyungpook National University, Daegu 41566, Korea

Abstract

A 14-year-old, spayed female, poodle was presented with dysuria and hematuria. A mass that appeared hypoechoic on ultrasound and hypoattenuating on computed tomography (CT) extended from the bladder neck to the urethra. Magnetic resonance imaging (MRI) showed the mass invading the muscular layer of the bladder, urethra, and prostate with distinct margins. Transitional cell carcinoma (TCC) was confirmed with the CADET-BRAF test. This study describes the CT and MRI features of suspected TCC lesions involving the bladder, prostate, and urethra. MRI showed superior soft tissue contrast resolution, enabling evaluation of invasion of the muscular layer of the bladder and urethra.

Keywords: computed tomography; magnetic resonance imaging; transitional cell carcinoma; urogenital neoplasm

Transitional cell carcinoma (TCC) is prevalent and highly invasive tumor of the urinary tract in dogs [1]. To determine appropriate treatment options and prognosis, it is important to assess TCC invasion into the bladder wall or neighboring organs [1–3]. According to the World Health Organization criteria, high T stage tumors that invade the bladder wall or neighboring organs at the time of diagnosis are considered negative prognostic factors [1]. Furthermore, in human medicine, muscular layer invasion of bladder TCC is assessed to determine treatment options and prognosis [3]. Another previous study of dogs has demonstrated that bladder TCC involving the urethra has a higher rate of distant metastasis at diagnosis and shorter survival time compared to bladder TCC without urethral involvement [4].

Ultrasonography (US) is a widely used modality for TCC evaluation in the urinary system, as it enables noninvasive real-time assessment without anesthesia [5]. However, TCC involving the caudal urethra may not be fully visualized due to the presence of the pubis or ischium [4]. Previous studies have demonstrated that computed tomography (CT) and magnetic resonance imaging (MRI) enable visualization of intrapelvic structures that are difficult to observe with US [6,7]. Furthermore, MRI and CT may be superior to US in terms of assessment of TCC invasion into the muscular layer [8]. Based on our review of the literature, no studies

have described the MRI features of TCC involving the urethra in dogs. The present study describes the features of suspected TCC lesions involving the bladder, prostate, and urethra in diagnostic imaging, including US, CT, and MRI.

A 14-year-old, spayed female, poodle dog weighing 4.9 kg was presented with a 2-week history of dysuria., hematuria, and dyschezia. Physical examination, complete blood count, and serum chemistry indicated no significant findings. Urinalysis revealed the presence of blood and abnormal transitional cells. Abdominal radiographs showed an irregular soft tissue opacity in the region of the urinary bladder (Fig. 1A). US (Prosound F75; Hitachi, Japan) revealed a wide-based, irregular, heterogeneous mass protruding into the urinary bladder and extending to the proximal urethra. A hyperechoic linear structure with weak acoustic shadowing was observed in the prostatic urethra (Fig. 1B). The acoustic shadowing from the pubic bone, led to the poor visualization of the caudal border of the mass and caudal intrapelvic urethra.

To assess the precise extent, invasion to surrounding tissue, and metastasis of the mass, a CT examination was performed with a 32-multislice CT system (Alexion; Canon Medical Systems, Japan). The dog was premedicated with butorphanol 0.2 mg/kg (Butophan Inj.; Myungmoon Pharm, Korea), and induced with propofol 5.0 mg/kg (Anepol Inj.; Hana Pharm, Korea) intravenously. General anesthesia was maintained with 2% isoflurane in oxygen delivered at a rate of 1.5 L/min. The dog was positioned in ventral recumbency on the CT table, and the scanning parameters used were as follows: 120 kV, 150 mA, 1.0 mm slice thickness, and 0.75 seconds rotation times. A contrast study was conducted after intravenous administration of 600 mgI/kg iohexol (Bonorex 300 Inj.; Daehan Pharm, Korea) injected 20 sec using an autoinjector (A-60; Nemoto Kyorindo Co., Japan). Post-contrast CT images of the arterial, portal-venous, and delayed phases were obtained at 20, 45, and 90 seconds after injection, respectively. A hypoattenuating ill-defined mass with an irregular margin, involving the bladder neck, prostate gland, and prostatic urethra was detected. The mass exhibited heterogeneous and weak contrast enhancement at the bladder neck and proximal urethra (Fig. 2). The wall in which the mass attached had intense, heterogeneous enhancement than the remainder of normal bladder wall on the portal-venous phase. However, muscular layer involvement was ambiguous and the mass from the surrounding tissue was not distinguished. Partial calcification of the mass at the prostatic urethra and enlarged right medial iliac lymph node with homogeneous contrast enhancement were also observed. There was no evidence of pulmonary metastasis.

Subsequently, an MRI examination was performed in a 1.5T MRI system (SIGNA Explorer; GE Healthcare, USA) using a

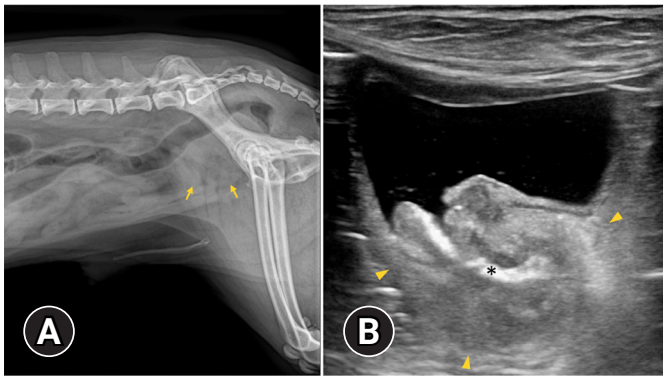

Fig. 1. (A) Lateral radiography of caudal abdomen and (B) ultrasonographic image of longitudinal view at the urinary bladder. On lateral radiography, the bladder is not seen, and an ill-defined heterogeneous soft tissue structure is observed at the bladder location (arrows). Ultrasonography shows a wide based heterogeneous mass at the bladder neck, extending to the proximal urethra (arrowheads). On ultrasonography, a hyperechoic linear structure with weak acoustic shadowing is observed in the prostatic urethra (asterisk). The caudal border of the mass and prostatic urethra is poorly visualized due to acoustic shadowing caused by the pubic bone.

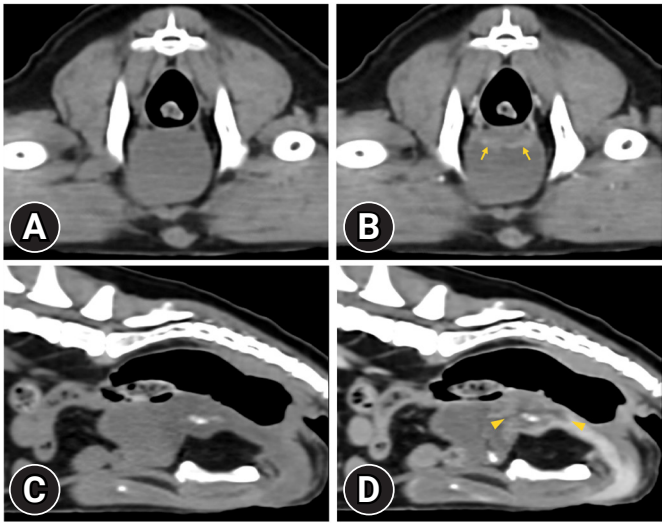

Fig. 2. Non-contrast (A) and portal-venous phase post-contrast (B) transverse computed tomography (CT) images and non-contrast (C) and portal-venous phase post-contrast (D) sagittal CT images. Hypoattenuating, ill-defined mass exhibits heterogeneous contrast enhancement and involves urethral opening and prostatic urethra (arrowheads). The bladder wall, to which the mass is attached, shows heterogeneous enhancement, but it is unable to differentiate the muscular layer from other layers of the bladder wall (arrows).

https://doi.org/10.14405/kjvr.20230041

combination of 16-channel flex coil (GE P/N 543000-3; GE Healthcare). The dog was positioned in dorsal recumbency on the MRI table under general anesthesia. MRI was performed, and sagittal T2-weighted (T2W) and T1-weighted (T1W) images of the caudal abdomen including the urinary bladder and urethra, were acquired. Post-contrast T1W images were obtained immediately after the intravenous administration of 0.15 mmol/kg gadoterate meglumine (Clariscan; GE Healthcare). The mass exhibited an irregular margin involving the bladder neck, prostate, and urethra and was heterogeneous with an isointense on T1W images (Fig. 3A), showing heterogeneous contrast enhancement (Fig. 3C) and a hyperintense on T2W images (Fig 3B and 3D). The mass invading the hypointense muscular layer of the bladder was detected at the bladder, disrupting the continuity of the hypointense muscular layer at the bladder neck on the T2W (Fig. 3B and D). On post-contrast T1W image, the hyperintense mucosal layer and hypointense muscular layer at the bladder neck was disrupted with the mass showing heterogeneous contrast enhancement (Fig. 3C). The normal urethral epithelium was hyperintense on the T2W, and isointense on the T1W image showed strong contrast enhancement. The caudal border of the mass was distinguishable due to a different contrast enhancement pattern from the urethral epithelium on the T2W and post-contrast T1W images (Fig 3B–D). The prostate parenchyma was heterogenous with hyperintense on the T2W image exhibiting heterogeneous contrast enhancement. The normal radial striations of the prostate were not identified, and the prostatic capsule was irregularly distorted. The right medial iliac lymph node enlargement was observed, but the lymph node was a homogeneously hypointense relative to surrounding fat on T1W image, isointense to surrounding fat on T2W image, exhibiting homogeneous contrast enhancement on the post-contrast T1W images, which was normal.

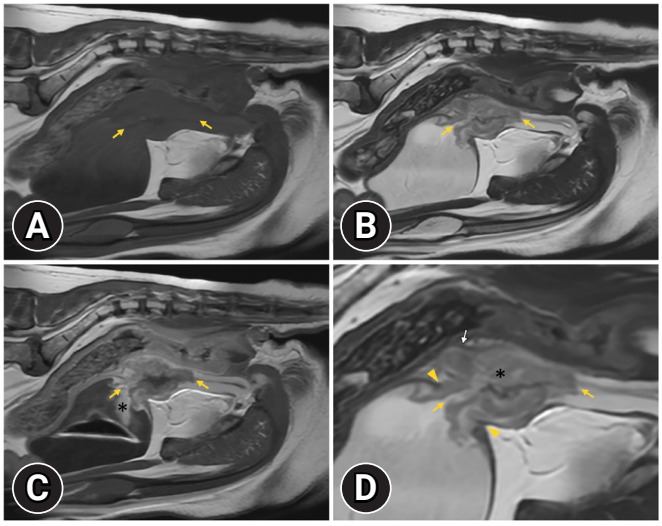

Fig. 3. T1-weighted (T1W) (A), T2-weighted (T2W) (B, D), and post-contrast T1W (C) sagittal magnetic resonance images. The mass involving the bladder neck and urethra is isointense on T1W (A, yellow arrows) and hyperintense on T2W (B, D; yellow arrows) and exhibits heterogeneous enhancement (C, yellow arrows). Disruption of the hypointense muscular layer continuity at the bladder neck by the mass is visible on T2W (D, yellow arrowheads). Prostatic parenchyma is abnormal on T2W (D, asterisk) and post-contrast T1W images. In addition, the prostatic capsule appears distorted (D, white arrow). The hyperintense area cranial to the bladder neck, seen on post-contrast T1W imaging, is thought to be caused by the retention of the contrast medium (C, asterisk).

Based on the diagnostic findings including US, CT, and MRI, TCC involving the bladder, prostate, and urethra was at the top of the list of differential diagnoses. The CADET-BRAF test, which examines the mutation of urothelial cells in the urine sample, was conducted. BRAF V595E mutation was confirmed in 6% of the urothelial cell. Although the origin of the tumor was not identified, based on the diagnostic imaging and CADET-BRAF, the dog was presumptively diagnosed as TCC involving the bladder, prostate, and urethra. The dog was treated with two cycles of mitoxantrone at a dose of 5 mg/m^2 and piroxicam 0.3 mg/kg SID. Because of myelosuppression, the chemotherapy protocol was altered to vinblastine at a dose of 1.5 mg/m^2 and piroxicam 0.3 mg/kg SID. No evident improvement was observed, and at 11 weeks after diagnosis, the dog was euthanized due to urinary tract obstruction and pelvic bone metastasis. An autopsy was not performed due to the owner's refusal.

This case report described US, CT, and MRI features of suspected TCC lesion involving the bladder, prostate, and urethra in a dog. MRI was found to be superior to other imaging modalities in evaluating TCC invasion of the bladder muscular layer. Furthermore, it was able to distinguish the normal urethral mucosal layer from the invading mass in the urethra and identify presumptive prostatic invasion with abnormal prostatic parenchymal change. These MRI findings are expected to facilitate the prognostic assessment of patients with bladder TCC.

Muscular layer invasion is a crucial staging criterion in urinary tract tumors and provides information for determining the prognosis and treatment options in human medicine [3]. Furthermore, invasion of the muscular layer was reported as a negative prognostic factor in dogs [1]. Invasion of the muscular layer was reported to be assessable by US [5]. However, in another study, the mass could be difficult to evaluate for muscular layer involvement in US due to the characteristics of the TCC,

which is located dorsally and calcified [8]. In the present study, muscular layer involvement was difficult to assess by US, due to the dorsal displacement of the urinary bladder and artifact of a calcified lesion within the mass. In the previous study about bladder TCC in dogs, muscular layer invasion could be assessed by CT, which shows irregular contrast enhancement of the bladder wall at an arterial phase in dual phase CT [8]. On the other hand, a human medicine study reported that CT is unable to accurately differentiate superficial invasion from deep muscle invasion and is only able to assess when the mass protrudes into the perivesical tissue [9]. In the present study, the bladder wall where the mass was located exhibited intense, heterogeneous enhancement compared with the normal bladder wall at a portal phase in triple phase CT. However, because the muscular layer of the bladder was not differentiated from other layers of the bladder wall, accurate diagnosis of muscular layer invasion was not obtained.

MRI was reported as an accurate modality for differentiating muscle- and non-muscle-invasive bladder cancer, in human studies [9,10]. In one study, MRI demonstrated sensitivity and specificity of 0.92 and 0.88, respectively, for differentiating muscular layer invasion [11]. In veterinary medicine, MRI, including T2W and post-contrast T1W images was reported to be able to detect invasion into the muscular layer in bladder TCC [7]. In the present study, considering previous studies and the dog's prolonged anesthesia time, sagittal T2W, T1W, and post-contrast T1W images were obtained. In this study, MRI was able to differentiate the mucosal and muscular layers of the bladder wall, which were not differentiated on CT. The mass invading the muscular layer, supported by the tumor disrupting the continuity of the hypointense muscular layer, was observed on the T2W and post-contrast T1W images. Multiparametric MRI, including T2W and dynamic contrast-enhanced MRI, is used in bladder tumors to differentiate muscular layer invasion with high diagnostic accuracy in human medicine [12]. Although it was not adopted in this study, an MRI protocol using multiparametric MRI may be applied in bladder tumors in dogs in further studies for a precise evaluation of muscular layer invasion.

Urethral and prostatic involvement is common in TCC [1]. Accurate diagnosis of urethral and prostatic involvement is crucial because it was reported to have a short survival time and a high metastasis rate at the time of diagnosis [1,4]. In the present study, the prostate exhibited hyperintense, heterogeneous parenchymal signal uniformity on the T2W image, with distortion of the prostatic capsule and radiating striations. This MRI finding is consistent with that of a previous study regarding prostatic tumors in dogs [10]. Although histopathological examination was not conducted in this study, it was possible to presumptively estimate the prostatic involvement of the mass on MRI. Shadowing from the pubic bone in US and low soft tissue contrast in CT can limit the evaluation of urethral involvement of TCC [7,10]. MRI provides superb soft tissue contrast, which enables the differentiation of urethral wall layering [13]. In the previous study, the urethra was observed with the inner mucosal and outer muscular layers on the T2W and post-contrast T1W images. The outer mucosal layer exhibited hypointense on T2W image, whereas the inner urethral mucosal layer showed hyperintensity on the T2W image and strong enhancement on the post-contrast T1W image [6]. In the present study, urethral layers were identified, which is consistent with the finding of the previous study. Due to superior soft tissue contrast on MRI, the exact margin of the mass was identified with a different signal intensity, which was distinguished from the hyperintense normal urethral mucosal layer. These findings suggest that MRI is superior to CT and US in assessing invasion of a urethral mass with high soft tissue resolution.

In conclusion, this study described the image findings of US, CT, and MRI in a dog with suspected TCC lesions involving the bladder, prostate, and urethra. MRI images, including T2W and post-contrast T1W sequences, enabled the evaluation of bladder muscular layer invasion. Furthermore, MRI detected involvement of urethra and prostate, which was not precisely identified by on CT. This study confirms that MRI is superior to CT in evaluating TCC lesions involving the bladder, prostate, and urethra.

ORCID

Wooseok Jin, https://orcid.org/0000-0003-2841-9236
Sang-Kwon Lee, https://orcid.org/0000-0002-3097-0345
Seulgi Bae, https://orcid.org/0000-0001-9487-5665
Taeho Oh, https://orcid.org/0000-0003-2898-6476
Kija Lee, https://orcid.org/0000-0002-4649-809X

References

1. Fulkerson CM, Knapp DW. Tumors of the Urinary System. In: Vail DM, Thamm DH, Liptak JM, eds. Withrow & MacEwen's Small Animal Clinical Oncology. 6th ed. pp. 645–656, Elsevier, St. Louis, 2020.
2. Knapp DW, Ramos-Vara JA, Moore GE, Dhawan D, Bonney PL, Young KE. Urinary bladder cancer in dogs, a naturally occurring model for cancer biology and drug develop-

https://doi.org/10.14405/kjvr.20230041

ment. ILAR J 2014;55:100–118.
3. Witjes JA, Bruins HM, Cathomas R, Compérat EM, Cowan NC, Gakis G, Hernández V, Linares Espinós E, Lorch A, Neuzillet Y, Rouanne M, Thalmann GN, Veskimäe E, Ribal MJ, van der Heijden AG. European Association of Urology guidelines on muscle-invasive and metastatic bladder cancer: summary of the 2020 guidelines. Eur Urol 2021;79:82–104.
4. Iwasaki R, Shimosato Y, Yoshikawa R, Goto S, Yoshida K, Murakami M, Kawabe M, Sakai H, Mori T. Survival analysis in dogs with urinary transitional cell carcinoma that underwent whole-body computed tomography at diagnosis. Vet Comp Oncol 2019;17:385–393.
5. Hanazono K, Fukumoto S, Endo Y, Ueno H, Kadosawa T, Uchide T. Ultrasonographic findings related to prognosis in canine transitional cell carcinoma. Vet Radiol Ultrasound 2014;55:79–84.
6. Cho Y, Choi H, Lee K, Lee Y. Magnetic resonance imaging evaluation of the prostate in normal dogs. J Vet Clin 2020;37:317–323.
7. MacLeod AG, Wisner ER. Computed Tomography and Magnetic Resonance Imaging of the Urinary Tract. In: Bartges J, Polzin DJ, eds. Nephrology and Urology of Small Animals. pp. 146–160, Blackwell Publishing Ltd., New Jersey, 2011.
8. Lee K, Choi S, Choi H, Lee Y. Clinical experience of MRI in two dogs with muscle-invasive transitional cell carcinoma of the urinary bladder. J Vet Med Sci 2016;78:1351–1354.
9. Kim B, Semelka RC, Ascher SM, Chalpin DB, Carroll PR, Hricak H. Bladder tumor staging: comparison of contrast-enhanced CT, T1- and T2-weighted MR imaging, dynamic gadolinium-enhanced imaging, and late gadolinium-enhanced imaging. Radiology 1994;193:239–245.
10. Yang NS, Johnson EG, Palm CA, Burton JH, Rebhun RB, Kent MS, Culp WT. MRI characteristics of canine prostatic neoplasia. Vet Radiol Ultrasound 2023;64:105–112.
11. Cornelissen SW, Veenboer PW, Wessels FJ, Meijer RP. Diagnostic accuracy of multiparametric MRI for local staging of bladder cancer: a systematic review and meta-analysis. Urology 2020;145:22–29.
12. Panebianco V, Barchetti F, de Haas RJ, Pearson RA, Kennish SJ, Giannarini G, Catto JW. Improving staging in bladder cancer: the increasing role of multiparametric magnetic resonance imaging. Eur Urol Focus 2016;2:113–121.
13. Ryu J, Kim B. MR imaging of the male and female urethra. Radiographics 2001;21:1169–1185.